Evaluation of the predictive capability of ionic liquid force fields for CH_4, CO_2, NH_3, and SO_2 phase equilibria

Utkarsh Kapoor, Atiya Banerjee, Jindal K. Shah

PII: S0378-3812(19)30120-7

DOI: https://doi.org/10.1016/j.fluid.2019.03.013

Reference: FLUID 12130

To appear in: *Fluid Phase Equilibria*

Received Date: 30 September 2018

Revised Date: 5 February 2019

Accepted Date: 18 March 2019

Please cite this article as: U. Kapoor, A. Banerjee, J.K. Shah, Evaluation of the predictive capability of ionic liquid force fields for CH_4, CO_2, NH_3, and SO_2 phase equilibria, *Fluid Phase Equilibria* (2019), doi: https://doi.org/10.1016/j.fluid.2019.03.013.

Evaluation of the Predictive Capability of Ionic Liquid Force Fields for CH_4, CO_2, NH_3, and SO_2 Phase Equilibria

Utkarsh Kapoor, Atiya Banerjee, Jindal K. Shah*

School of Chemical Engineering, Oklahoma State University, Stillwater, OK 74078 USA

Abstract

Molecular dynamics simulations were performed to systematically compare four all-atom classical ionic liquid force fields and provide recommendations for the appropriate selection of an ionic liquid force field for the calculation of Henry's constants of gases. Four solutes of varying polarity, viz., CH_4, CO_2, NH_3 and SO_2 were investigated. The ionic liquids considered in this work contain the same cation,1-n-butyl-3-methylimidazolium $[C_4mim]^+$ paired with four different anions chloride Cl^-, methylsulfate $[MeSO_4]^-$, dicynamide $[DCA]^-$, and bis(trifluoromethanesulfonyl) imide $[NTf_2]^-$. The calculations were performed at three temperatures of 333, 353, and 373 K to enable the computation of enthalpies and entropies of absorption. Based on a comparison of the predicted results with those available in the literature, it was observed that the recently developed virtual-site ionic liquid force field tends to exhibit an overall better agreement with the published data in comparison to other force fields. Our results further indicate that, in general, SO_2 is the most soluble gas due to the strongest interaction with ionic liquids, followed by NH_3, CO_2 and CH_4.

Keywords: Molecular Dynamics, Ionic Liquids, Force Fields, Henry's Constants, Bennett Acceptance Ratio (BAR)

---

*Corresponding author
Email address: `jindal.shah@okstate.edu` (Jindal K. Shah)

1. Introduction

Ionic liquids are a special class of electrolytes that are characterized by remarkable properties such as low volatility, high thermal stability, wide electrochemical window, and excellent solvation strength. [1, 2] Such favorable properties have enabled their usage in diversity of applications ranging from energy storage [3, 4], reaction media [5, 6], battery electrolytes [7, 8, 9], electroplating [10, 11], solar cells [12, 13, 14], to gas separation processes. [15, 16, 17, 18] One of the most attractive features of these fluids is that a large number of ionic liquids with desired properties can be envisioned through cation-anion combinations. [19] Another avenue for increasing the number of ionic liquids is through blending two ionic liquids to precisely tune properties required for a particular application. [20, 21, 22, 23] Although conceptually a simple and promising approach, the myriad of ionic liquids makes it virtually impossible to experimentally screen ionic liquids for their properties. To address this, molecular simulations have been carried out as a complementary to experiments in understanding structure-property relationships, estimate properties, and understand molecular level mechanisms responsible for various phenomena over the last two decades.

The predictive capability of classical molecular simulation-based methods critically depends on an accurate description of intramolecular and intermolecular interactions in ionic liquids. Towards this end, a lot of effort has been expended to parametrize various classical non-polarizable force field models for estimating pure component thermophysical properties. Notable examples of all-atom force fields for imidazolium-based ionic liquids include those published by Canongia Lopes and Pádua [24, 25, 26, 27], Acevedo and co-workers [28, 29, 30], Ludwig and co-workers [31, 32] and Maginn and co-workers. [33, 34, 35, 36, 37] The first generation of ionic liquid force fields were derived based on placing integer charges on the ionic liquid ions. Transport properties of ionic liquids obtained with these force fields were found to be lower than the corresponding experimental measurements. In order to remedy this situation, the application of scaled charge models has received increasing attention as a way to account for the polarization in ionic liquids. Adoption of this approach has been demonstrated to considerably improve the agreement between simulation and experimental results for transport properties.

Although ionic liquid force fields have been routinely refined to reproduce their thermophysical properties, the testing of these force fields for phase equilibria properties is not fully developed. This is surprising given that a large number of ionic liquid applications necessitate the knowledge of phase equilibria. For example, in the seminal paper, Blanchard and Brennecke demonstrated the ability of the ionic liquid 1-n-butyl-3-methylimidazolium [C_4mim] hexafluorophosphate [PF_6] to dissolve high amounts of CO_2. [38] Since then ionic liquids have been under intense scrutiny for their applications as gas separating agents with numerous experimental measurements of solubility of various gases being carried out. For example, the solubility of CO_2 [39, 40, 41], SO_2 [42, 43, 44], H_2 [39, 41], O_2 [45, 40], H_2S [46, 47], NH_3 [48, 49, 43, 50], CH_4 [15, 40, 41], C_2H_6 [15, 40, 41] in ionic liquids has been extensively studied over the past few years. A comprehensive set of experimental data related to the gas solubility in ionic liquids was published by Chen and co-workers. [18]

Molecular simulations have also been conducted to predict solubility of CO_2 [51, 52, 53, 54, 55, 56, 57, 58], CH_4 [56, 52, 51, 56, 57, 58], NH_3 [59, 60], and SO_2[54, 58] in ionic liquids. The phase equilibria properties of gases in these studies were computed by a combination of an ionic liquid force field and available interaction potential for the gases. Despite these studies, the information on how the choice of an ionic liquid force field affects the phase equilibria predictions is far from known. We are aware of only one simulation study by MarinRimoldi et al. [61] in which a critical evaluation of several popular force fields was undertaken for three ionic liquids [C_4mim] chloride Cl, [C_4mim][PF_6], and [C_4mim] bis(trifluoromethanesulfonyl)imide [NTf_2] for computing water solubility. The authors concluded that the experimentally measured absorption isotherms could not be satisfactorily reproduced by any of the force fields examined and force fields taking into account the polarization and charge transfer are necessary. Similar studies are desirable for identifying a suitable ionic liquid force field for their ability to accurately describe ionic liquid-solute interactions.

In this article, we attempt to bridge the gap in the knowledge by investigating four all-atom ionic liquid classical force fields, (i) one developed by Canongia and Padua - designated as CL&P, [26] and (ii) three put forth by Acevedo and co-workers - represented as (a) OPLS2009, [28] (b) OPLS2009_0.8 (with scaled charges) [29] and (c) Virtual site ionic liquid (VSIL) [30]. We present gas solubilities in the form of Henry's constant for four gases: (i) nonpolar CH_4; (ii) quadrupolar and acidic CO_2; (iii) polar and basic NH_3; (d) polar and acidic SO_2. The selection of these gases is driven by various intermolecular forces that are responsible for their dissolution in ionic liquids. Furthermore, their solubilities range from high (NH_3 and SO_2), moderate (CO_2), and low (CH_4). The four ionic liquids considered in this work contain the common cation $[C_4mim]^+$ and different anions Cl^-, methylsulfate $[MeSO_4]^-$, dicyanamide $[DCA]^-$, and $[NTf_2]^-$. These ionic liquids are characterized by various hydrogen bonding strengths between the cation and anion in the order $Cl^- > [MeSO_4]^- > [DCA] > [NTf_2]^-$. [62, 63] The Henry's constants were evaluated by computing the infinite dilute excess chemical potential of gases 333, 353, and 373 K. A comparison between predicted values for the Henry's constants, heat of absorption, and entropy of absorption obtained in this work and experimental/simulation literature values is also included. The literature values are either directly obtained from the studies, whenever available, or are extrapolated from the temperature dependent data. All the relevant data are also listed in the supporting information.

2. Force Field

In general, in an all-atom classical force field, the total energy of the system is represented as the combination of intermolecular energies (electrostatic and van der Waals interactions), and intramolecular energies, i.e., bond stretching, angle bending, torsion (both proper and improper). The force field generally assumes the following functional form:

$$\begin{aligned} E_{\mathrm{tot}} &= \sum_{ij}^{\mathrm{bonds}} \frac{k_{r,ij}}{2}(r_{ij} - r_{0,ij})^2 + \sum_{ijk}^{\mathrm{angles}} \frac{k_{\theta,ijk}}{2}(\theta_{ijk} - \theta_{0,ijk})^2 \\ &+ \sum_{ijkl}^{\mathrm{torsions}} \sum_{m=1}^{4} \frac{k_{m,ijkl}}{2}[1 + (-1)^{m+1} \cos(m\phi_{ijkl})] + \\ &+ \sum_{ij}^{\mathrm{nonbonded}} \left\{ 4\epsilon_{ij} \left[\left(\frac{\sigma_{ij}}{r_{ij}}\right)^{12} - \left(\frac{\sigma_{ij}}{r_{ij}}\right)^{6} \right] + \left(\frac{q_i q_j}{r_{ij}}\right) \right\} \end{aligned} \tag{1}$$

where the adjustable parameters $k_{r,ij}$, $k_{\theta,ijk}$, $k_{m,ijkl}$, σ and ϵ have the usual meaning and are unique for different force fields.

Four ionic liquids containing cation 1-n-butyl-3-methylimidazolium $[C_4mim]^+$ combined with anions chloride Cl^-, methylsulfate $[MeSO_4]^-$, bis(trifluoromethanesulfonyl)imide $[NTf_2]^-$, and dicynamide $[DCA]^-$ were modeled with the following force fields: (1) Simulations using force field parameters of Canongia Lopes-Pádua [26, 27] will be abbreviated as CL&P and black color will be used to represent the results in graph; (2) Since CL&P force field was parameterized based on the OPLS-AA force field, simulations were also conducted using OPLS2009 force fields, [28] represented by green color in the graphs. It is to be noted that total charge on an ion is ±1 for these force fields; (3) It is well established that use of non-integer charges on ions can be used as an effective strategy to improve the dynamical property predictions as it can, in part, account for the polarizability. Therefore, in order to evaluate the effect of scaled charges on the calculated properties simulations using OPLS2009_0.8 with ion charges scaled to ±0.8 were conducted, [29] blue color will be used to represent the results graphically; (4) Recently, Acevedo and co-workers [30] refined their OPLS-AA force fields for imidazolium-based ionic liquids by placing a virtual site at the bisector of two ring nitrogens, which was able to predict properties such as experimental densities, heat of vaporizations, heat capacities, viscosities, surface tensions, and self-diffusivities along with cation-anion hydrogen bonding and π-π cation-cation stacking with a high degree of accuracy. The total charge on the ion is ±0.8. Simulations with this force field will be abbreviated as VSIL and be displayed in red color on the graph. For all the four force fields, the unlike Lennard-Jones interactions were computed by the geometric-mean combining rule for both the Lennard-Jones interaction parameters. The intramolecular 1-4 nonbonded interactions (Lennard-Jones and electrostatics) were reduced by a factor of 2, while these interactions were not computed for atoms involved in bonded interactions (bonds and angles). The force field parameters for CO_2, SO_2 and NH_3 were obtained from the respective works of Shi and Maginn [64, 65, 59], while TraPPE-UA parameters were used to model CH_4. [66]

3. Simulation Details

Molecular dynamics (MD) simulations, using GROMACS 5.1.5 package [67, 68], were carried out at a pressure of 1 bar and three different temperatures 333, 353, and 373 K. Gas solubility of CH_4, CO_2, NH_3 and SO_2 the ionic liquids was expressed in terms of the Henry's constant, which was evaluated using four different classical force fields (see Force Field section). As these gases dissolve in ionic liquids via physical absorption mechanism, the use of Henry's constant is justified. Further, the Henry's constants provide direct information on the solute-solvent interactions. Assuming infinite dilution limit of the solute, the Henry's constants, k_H, were obtained by the following expression:

$$k_H = \rho RT \exp\left(\frac{\mu^{ex}}{k_B T}\right) \tag{2}$$

where ρ is the molar density of the solvent without the solute dissolved in it, and T is the temperature of interest. The symbols R and k_{B} refer to the universal gas constant and the Boltzmann's constant, respectively. The excess chemical potential μ^{ex} was determined using Bennett's Acceptance Ratio (BAR) [69] approach. In this approach, the solute-solvent interaction strength was varied via a coupling parameter λ and an independent MD simulation was conducted at each λ point. Then, the free energy change between subsequent λ's was evaluated using GMX BAR utility of GROMACS, and the total change in free energy was determined by taking the sum over all λ values.

For CO_2, SO_2, and NH_3, a two-stage strategy was adopted. In the first stage, only the Lennard-Jones interactions were scaled from the ideal gas state to a solute with Lennard-Jones parameters identical to those given by the force field. The transformation was accomplished in 11 λ points evenly spaced between 0 and 1. The next step involved coupling electrostatic interactions of the gases to the ionic liquid system in eight stages (λ = 0.1, 0.2, 0.4, 0.6, 0.7, 0.8, 0.9 and 1.0) holding the Lennard-Jones parameters fixed. For CH_4, a single-stage scheme of coupling the Lennard-Jones interactions was followed as the united-atom TraPPE force field for CH_4 does not contain charges.

The initial configurations were generated using PACKMOL [70] by inserting 1 molecule of gas and 256 ion pairs for an ionic liquid in a cubic box with periodic boundary conditions. The initial box sizes were estimated based on experimental densities of pure ionic liquids. These initial configurations were subjected to a steepest descent minimization followed by a 2 ns annealing scheme in which the temperature was iteratively raised to a temperature 200 K above the desired temperature before bringing it back to the target temperature. Using langevin dynamics integrator, additional relaxation of each system was achieved by simulating the systems in canonical (NVT) and isothermal-isobaric (NPT) ensembles for 5 ns and 20 ns respectively. This was followed by a production run of 20 ns in the NPT ensemble. All the simulations were performed with a time step of 1 fs. During production run, the temperature and pressure were controlled using Nosé-Hoover thermostat and Parrinello-Rahman barostat, respectively, with coupling time constants of τ_T = 0.4 ps and τ_P = 2.0 ps. Appropriate tail corrections were applied for the nonbonded Lennard-Jones interactions while electrostatic interactions were handled using Particle mesh Ewald (PME) method, each with a potential cutoff of 16 Å. Statistical uncertainties were estimated from three independent simulations initiated from different starting configurations.

4. Results and Discussion

The primary goal of the present work is to test the performance of four different force fields for phase equilibria property predictions of various gases with solubilities ranging over several orders of mangitude in different ionic liquids. From equation 2 it is clear that, at a given temperature, the value of Henry's constant primarily depends on two factors: (i) density of the pure solvent (ionic liquid in this work), and (ii) excess chemical potential of the gas dissolved in ionic liquid at infinite dilution. Therefore, accurate reproduction of liquid phase densities of pure ionic liquids can be used as a test to assess the performance of a force field model. Figure S1 of the supporting information shows the temperature dependent variation of densities obtained for [C_4mim]Cl, [C_4mim][$MeSO_4$], [C_4mim][DCA], and [C_4mim][NTf_2] ionic liquids using four different classical force fields examined in this work. A direct comparison of the predicted values with the experimental and simulation-based literature data indicates that, in general, all the force fields are able to estimate the liquid densities with good accuracy with maximum deviation of ~3 % considering the statistical uncertainties. Given the generality and transferability of the force field models considered here, accuracy within ±3 % deviation can be considered reasonable. In fact, Canongia Lopes and Pádua [24, 25, 26, 27], and Acevedo and co-workers [28, 29, 30] reported densities of these ionic liquids with similar accuracies. However, a closer inspection suggests that force fields with scaled charge models (VSIL and OPLS2009_0.8) leads to better predictions of the temperature dependent-density trends.

Acevedo and co-workers [29] reported that although OPLS2009 can predict properties such as heat of vaporizations, heat capacities, viscosities, surface tensions, and self-diffusivities reasonably well, a charge scaling improves reproduction of not only the bulk-solvent properties but also the local ion–ion intermolecular interactions such as cation-anion hydrogen bonding and π-π cation-cation stacking, in imidazolium-based ionic liquids, with maximum absolute error ranging between 10-15 %, as was observed in OPLS2009_0.8. Furthermore, presence of a virtual-site, in VSIL model, dramatically improves the above mentioned macroscopic with a high degree of accuracy with maximum absolute error of < 3.5 % for all except self-diffusion coefficients where deviation was ~10 %. [30] Structural properties were also commensurate with those calculated from ab initio calculations. Thus, overall the four force fields considered here can predict the structural and macroscopic properties of pure ionic liquids with good accuracy.

4.1. Gas Solubilities in terms of Henry's constants

Before delving into the comparison, it is worth mentioning some general apparent trends. (i) For a given gas and an ionic liquid, the Henry's constants increase with increasing temperature, implying that the solubility of the gas decreases. (ii) At a particular temperature, for the same ionic liquid the solubility follows the order: $SO_2 > NH_3 > CO_2 > CH_4$. This trend is consistent with previously reported trend. [18] These trends are well-reproduced irrespective of the choice of force field model. However, important differences between the performances of the force fields, in terms of the level of agreement reached with the experimental data, will be discussed in the following sections. The following subsections are organized in the increasing order of gas solubilities.

4.1.1. CH_4 Solubility

The variation in Henry's constants of CH_4 for the ionic liquids and force fields considered in this work is given in Figures 1 (a) - (d). These predictions have been compared with the published experimental data. To our knowledge, a complete set of data for the imidazolium-based ionic liquid containing butyl side chain throughout the temperature range of 333-373 K is not available for the current set of anions. Hence, comparison is made at discrete temperature levels. As remarked earlier, CH_4 is the least soluble in ionic liquids amongst all the gases examined in this work. This is clearly reflected in the calculations performed, where $k_{H,\mathrm{CH4}}$ is an order of magnitude higher than the Henry's constants for CO_2, NH_3 and SO_2.

For [C_4mim]Cl ionic liquid, significant difference in the predictions using different force fields are observed at 333 K. The Henry's constants of CH_4 calculated with the OPLS2009 and CL&P force fields are lower by a factor of 4 when compared with those computed with the force fields with scaled charges (VSIL and OPLS2009_0.8). In general, the Henry's constants for methane are similar when scaled charge force fields are employed and are higher than those obtained with the force fields developed with integer charges. Our calculations (not shown) of the Henry's constant of CH_4 in [C_4mim]Cl using a united-atom force field with ionic charges of ±0.8 also indicate solubilities similar to those obtained with the OPLS2009_0.8 and VSIL force fields. At the highest temperatures, all the force fields yield similar values within the statistical uncertainties. Interestingly, the OPLS2009_0.8 and VSIL force field show almost no variations in the Henry's constants. We will revert to this point below when discussing the heat of absorption for various systems.

The force field performance is qualitatively different for the [C_4mim][$MeSO_4$] ionic liquid. In terms of matching the Henry's constant with experimental results (Figure 1(b)), the CL&P and OPLS2009 force field outperform the OPLS2009_0.8 and VSIL at 333 K. At a temperature of 353 K, the Henry's constant computed with the OPLS2009 force field is in better agreement with the experimental results, while the scaled charge force fields are to be preferred at 373 K. In terms of the temperature variation, the OPLS2009_0.8 and VSIL force fields reproduce the experimental trend. Similar to the observation for [C_4mim]Cl, the Henry's constants predicted with the OPLS2009_0.8 and VSIL force fields are nearly indistinguishable, especially at 333 and 353 K.

The Henry's constants for [C_4mim][DCA] are presented in Figure 1(c). When a comparison is made between various force fields, the OPLS2009_0.8 force field predicts values that are the lowest at all the temperatures, implying the largest solubility with the Henry's constants ~ 1100 bar. The VSIL force field yields values that are nearly independent of the temperature (~ 1750 bar). The higher values for the Henry's constant in the case of the VSIL force field may be related to a higher density obtained for the pure ionic liquid than that with the OPLS2009_0.8 force field. It is interesting to note that the Henry's constants estimated by fitting the soft-SAFT equation of state to the experimental data and determining the slope as the solubility approaches zero [71] fall between the predictions by the OPLS2009_0.8 and VSIL force fields. Additionally, the weak temperature dependence of the Henry's constants for CH_4 is well described by the two force fields. The CL&P and OPLS2009 force field overestimate the Henry's constants over the three temperatures in comparison to those experimentally derived and calculated from the scaled charge models. It is noteworthy that the OPLS2009 force field is able to reproduce the temperature invariance of the Henry's constants. According to our calculations, an incorrect temperature trend of the Henry's constant is likely to be obtained with the CL&P force field.

For the [C_4mim][NTf_2] ionic liquid, OPLS2009_0.8 force field is in very good agreement with the available experimental results [72] and group contribution [73] predictions by Yu and co-workers at 333 and 353 K and is observed to perform the best in comparison to other force fields. At 333 K, the Henry's constant of 497 ± 17 bar obtained from this force field is also comparable to Henry's constant of 524 bar reported by Ramdin and co-workers [57] from Monte Carlo simulations and 549 bar from experiments by Peters and co-workers. [74] On the other hand, Budhathoki et al. [51] determined the Henry's constant of CH_4 to be 331 ± 11 bar from Monte Carlo simulations, the value which is quantitatively obtained with the VSIL force field (339 ± 7 bar). The VSIL force field consistently yield the highest solubilities for CH_4 followed by OPLS2009_0.8. For these two force fields, the Henry's constants are within a factor of 2 at all the temperatures. The CL&P force field also appears to capture the solubility trend with the temperature.

Overall, based on the available data and our predictions, for [C_4mim]$^+$ system, the CH_4 solubility order can be expressed as [NTf_2]$^-$ ~ [$MeSO_4$]$^-$ > [DCA]$^-$ > Cl^-. Comparing the experimental data with the simulation predictions, the VSIL and OPLS2009_0.8 force fields appear to reproduce the experimental data reasonably well for [C_4mim][DCA] and [C_4mim][NTf_2]. No single force field can be identified for predicting accurately the Henry's constant of CH_4 in [C_4mim][$MeSO_4$].

4.1.2. CO_2 Solubility

Figures 2 (a) - (d) depict the behavior of Henry's constants of CO_2 for the ionic liquids [C_4mim]Cl, [C_4mim][$MeSO_4$], [C_4mim][NTf_2] and [C_4mim][DCA] as a function of the temperature for each of the force fields. Experimental data are also included for comparison. In general, the CO_2 solubility is predicted to follow the order [NTf_2]$^-$ > [DCA]$^-$ > [$MeSO_4$]$^-$ > Cl^- at all the temperatures. Deviations from this trend were observed at the lowest temperature (333 K) with the CL&P ([NTf_2]$^-$ > Cl^- > [DCA]$^-$ > [$MeSO_4$]$^-$) and OPLS2009 (Cl^- > [NTf_2] > [$MeSO_4$]$^-$ ~ [DCA]$^-$) force fields. The overall trends for the CO_2 solubility is consistent with the hydrogen-bond acceptor ability of the anions when they are combined with the same cation. [62, 63] This result was expected as it is well established fact that solubility mechanism of CO_2 in ionic liquids is highly dependent on the interaction between CO_2 and anion and the size with weakly coordinating anion possessing greater absorption capacity. [18]

For [C_4mim]Cl (Figure 2 (a)), it is evident that the Henry's constant predictions are similar for all the force fields when statistical uncertainty are taken into account. Moreover, the agreement with the experimental data [75] is also good. It is noteworthy that the Henry's constants obtained with the OPLS2009, OPLS2009_0.8 and VSIL force fields are in excellent agreement with the calculations performed with a united-atom model with scaled charges. [76] At 333 K, the Henry's constants calculations with VSIL and OPLS2009_0.8 are show a good level of agreement with experimentally measured Henry's constant, while the CL&P and OPLS2009 predictions are lower by approximately 50 %. This is probably attributable to the fact that melting temperature of [C_4mim]Cl is ~ 340 K, making it a super-cooled liquid at 333 K. In addition, the high viscosity of the ionic liquid makes it challenging to measure CO_2 solubility. At the highest temperature (373 K), all the force fields converge around the experimental measurement.

In [C_4mim][$MeSO_4$], trend opposite to [C_4mim]Cl is observed (Figure 2 (b)), i.e., at lowest temperature of 333 K, the predicted Henry's constants using all the force fields are comparable to the experimentally reported values. [77, 78, 79] As the temperature is increased to 353 K and 373 K, CL&P and OPLS2009 force field predicts Henry's constants almost 1.5 times the values predicted by VSIL and OPLS2009_0.8. Moreover, considerable differences can also be observed for the values obtained from the experimental studies of Kumelan et al. [77] and Bahadur et al. [78] at the respective temperatures. Therefore, it is difficult to use experimental measurements as a benchmark to test the predictions from different force fields. Nevertheless, VSIL predicts values with significantly low standard deviations at all the temperatures. Thus, it seems prudent to employ the force field for modeling the CO_2 interactions in this ionic liquid.

For CO_2 solubility in the [C_4mim][DCA] ionic liquid, experimental data collected by Carvalho et al. [80] at all the three temperatures are used to gauge the accuracy of the various force fields; the VSIL and CL&P force field closely resemble the experimental data. The OPLS2009 force field overpredicts the Henry's constants while values lower than the experimental data are obtained when OPLS2009_0.8. All the force fields are able to reproduce the temperature variation that is consistent with the experimental data.

Considering [C_4mim][NTf_2], which is probably the most studied and well-parameterized ionic liquid, all the four force fields give different values at a given temperature (see Figure 2 (d)). In general, the VSIL force field predicts highest CO_2 solubility in [C_4mim][NTf_2] ionic liquid followed by OPLS2009_0.8, OPLS2009 and CL&P respectively. VSIL agrees very well with experimentally measured values reported by Carvalho et al. [80], Lee et al. [81], Jacquemin et al. [39] and Hiraga et al. [82]. While values predicted by CL&P and OPLS2009 are in agreement with those reported by Raeissi et al. [83]. One possible explanation for the difference in experimentally determined values may be related to the presence of impurities such as Cl^- and water. [84] Also, the use of different experimental methods/protocols can produced different values. [18] The predictions with the VSIL force field compare well with the values determined by Kapoor and Shah [76] who used a united-atom model force field proposed by Liu et al. [85] Further, these values also correspond well to those reported by Budhathoki et al. [51] and Singh et al. [52] who employed a Generalized Amber Force Field for their Monte Carlo simulations. Although the predicted values of Henry's constants are different, we concluded that, significantly lower statistical uncertainties and excellent agreement with most of the experimental and simulation-based studies indicate that the recently proposed VSIL force field is a reliable force filed for determining CO_2 solubility in [C_4mim][NTf_2].

4.1.3. NH_3 Solubility

Henry's constants of NH_3, as a function of temperature, the four ionic liquids and different force fields are displayed in Figures 3 (a) - (d). To the best of our knowledge, experimental and simulation-based literature data are reported for the ionic liquids examined. However, it is interesting to note that all the ionic liquids exhibit comparable Henry's constants, ranging from 10 to 50 bar at the three temperatures investigated. Such a behavior suggests that, unlike CO_2, the anion effect on NH_3 solubility is less pronounced. This observation is consistent with the study performed by Shi and Maginn [59] in which the authors computed the radial distribution functions of NH_3 with the cation and anion of the ionic liquid ethylmethylimidazolium [C_2mim][NTf_2] and concluded that the most important NH_3 interaction occurred with one of the hydrogen atoms in the imidazolium ring. Based on the activity coefficients and vapor pressure data provided in this paper, we estimated the Henry's constants for NH_3 in [C_2mim][NTf_2] to be 11.9, 22.9 and 51.0 bar at 298.1, 322.3, and 347.5 K, respectively. These values are similar to the force field predictions, but somewhat lower, presumably due to the longer alkyl chain employed in this study. Furthermore, Henry's constants data extrapolated from the available experimental measurements for [C_4mim][BF_4] and [C_4mim][PF_6] [49] lie between 10 tand 30 bar for the range of temperature studied here. In fact, comparison of Henry's constants for [C_2mim][BF_4] and [C_2mim][NTf_2] obtained from the works of Li et al. [50] and Yokozeki and Shiflett [49] respectively, indicate similar NH_3 solubility.

As far as the performance of four force fields is concerned, trends similar to CO_2 solubility are observed. For instance, predictions obtained by CL&P force field and OPLS2009 are similar while VSIL and OPLS2009_0.8 track each other for three ionic liquids: [C_4mim]Cl, [C_4mim][[$MeSO_4$], and [C_4mim][DCA]. Considering absolute values, the CL&P force field or OPLS2009 exhibit solubilities that are higher than the corresponding solubilities estimated by the other two force fields for these three ionic liquids. Contrary to this observation, all the force fields but OPLS2009_0.8 display very similar NH_3 solubilities in [C_4mim][NTf_2]. As there is no strong dependence of the Henry's constant on the type of force field, any of the four force fields is suitable for the initial estimate. If the force fields are ranked based solely on the precision, VSIL force field is found to be superior.

4.1.4. SO_2 Solubility

The dependence of Henry's constants of SO_2 for various ionic liquids on the type of force field is illustrated in Figures 4 (a) - (d). The Henry's constants span the range from 1-20 bar, with higher values observed at higher temperatures. Across all the ionic liquids, we observe that the Henry's constants are categorized in two force field groups: (1) CL&P and OPLS2009; (ii) VSIL and OPLS2009_0.8. For the ionic liquids [C_4mim][$MeSO_4$], [C_4mim][DCA], and [C_4mim][NTf_2], the VSIL and OPLS2009_0.8 force fields produce Henry's constants lower than those calculated with the other two force fields. A reversal in the trend is evident for the [C_4mim]Cl.

The available literature data are sparse for SO_2 Henry's constant in these ionic liquids; however, comparison of experimental and other simulation data at different temperatures is performed to test the validity of the force fields. The experiments by Lee et al. [86] show that the absorption of SO_2 is higher in [C_4mim]Cl in comparison to that for [C_4mim][$MeSO_4$] at 323 K (Henry's constant 0.55 bar, see below). However, the absorbed amount could not be fully recovered hinting at a chemical complex formation. The value of 0.9 bar obtained with the OPLS2009 and CL&P force fields at 333 K seem to follow this behavior. As the possibility of chemical interactions in the models is neglected, the agreement can be considered somewhat fortuitous. The Henry's constant calculations using a free energy-based molecular modeling approach by Mondal and Balasubramanian [87] also point to a value of 1.0 bar at 353 K, which is closely mimicked by the OPLS2009 and CL&P force fields for this ionic liquid. VSIL and OPLS2009_0.8 force field estimations for the Henry's constants are in line with the physical absorption mechanism for SO_2.

Shiflett and Yokozeki [44] derived a Henry's constant of 0.04 bar for [C_4mim][$MeSO_4$] at 298 K. The authors alluded to the chemical complexation between SO_2 and the ionic liquid. The data reported by Lee et al. [86] over the temperature range of 308-328 K show that the Henry's constant of SO_2 in this ionic liquid varies from 0.43 to 0.62 bar, indicating that the solubility of SO_2 is most likely driven by a chemical complexation mechanism. Higher temperatures and modeling the physical solubility are the main reasons that the Henry's constants predictions for SO_2 are higher than than those reported experimentally. The predictions with VSIL and OPLS2009_0.8 closely follow one another at all the temperatures with similar behavior noted for the other two force fields.

In the case of [C_4mim][DCA], there exists only one data point reported by Garcia et al. [88] based on COSMO-RS calculations at 298 K. Although a direct comparison is not possible due to the different modeling approaches and temperatures, the Henry's constant values determined in this work are similar. Interestingly, the accuracy of the predictions for all the force fields is remarkably similar for [C_4mim][NTf_2]. The COSMO-RS calculations performed by Garcia et al. [88] at 303 K yield a value of 3.5 bar for the Henry's constant of SO_2 in [C_4mim][NTf_2], which compares favorably with the data reported here. Anderson et al. [89] measured the Henry's constant of SO_2 in 1-

hexyl-3-methylimidazolium [C_6mim][NTf_2] to be ~ 4.1 bar at 333 K. Shi and Maginn [90] calculated this value to be 3.6 bar from the absorption isotherms determined from Monte Carlo simulations. Given that the effect of the alkyl chain length on the SO_2 solubility is minor [91], the Henry's constant predictions for all the force fields are in very good agreement for [C_4mim][NTf_2].

4.2. Enthalpies and Entropies of Absorption

The partial molar enthalpy (Δh) of absorption is useful in understanding the strength of interaction between the solute and solvent, while the partial molar entropy (Δs) of absorption provides insights into the degree of ordering in liquids associated with the dissolution of the solute. These thermodynamic quantities can be extracted from the temperature-dependent Henry's constant data using equations 3 and 4

$$\Delta h = R\left(\frac{\partial(\ln\ k_{\mathrm{H}})}{\partial(1/T)}\right)_P \tag{3}$$

$$\Delta s = -R\left(\frac{\partial(\ln\ k_{\mathrm{H}})}{\partial(\ln\ T)}\right)_P \tag{4}$$

The values of Δh and Δs for all the gases in different ionic liquids along with the literature data - wherever available - are collected in Tables 1 and 2 respectively.

With the exception of few cases, the values of Δh are negative as the solubility of all the gases were found to decrease with increasing temperatures. In general, all Δh values are relatively small, irrespective of the gas and ionic liquid, indicating a physical dissolution mechanism as the absorption driven by chemical interaction would yield much larger values. [40] The interactions strengths for the gases with ionic liquids increase in the order of CH_4 < CO_2 < NH_3 < SO_2. This observations can be explained on the basis of the type of interactions the solute is able to establish with ionic liquids. Table 3 lists the polarizabilities and dipole and quadrupole moments of the gases. This clearly suggests that the primary mode of interaction for CH_4 is van der Waals (vdW) interactions due to its nonpolar character. In addition to the vdW interactions, CO_2 can interact through electrostatic interactions due to its large quadrupole moment. The polar nature of NH_3 and SO_2 is evident due to the presence of permanent dipole and quadrupole moments which is also reflected in the high enthalpy of absorption. The partial molar entropy of absorption follows exactly the opposite trend to that for the enthalpy. The strength of the interaction also correlates with the order of increasing gas solubility.

4.2.1. CH_4

In line with the variation in Henry's constants with temperature, the calculated enthalpy of absorption values are negative except for [C_4mim][DCA] ionic liquid with the CL&P force field, indicating that the solubility decreases as the temperature is raised. The enthalpies are rather low (ranging from -5 kJ/mol to 0 kJ/mol) for all the ionic liquids when computed using the VSIL and OPLS2009_0.8 force fields, implying a weak interaction with the ionic liquids and temperature dependence of solubility. The OPLS2009 force field shows such a weak dependence only for [C_4mim][DCA], while the CL&P force field produces this trend only for [C_4mim][NTf_2] and [C_4mim][DCA]. These force fields, however, suggest a strong temperature dependence for methane solubilities for [C_4mim]Cl and [C_4mim][$MeSO_4$] as can be judged from the enthalpy values in Table 1. Comparing the enthalpy of absorption with the available literature data shows that the VSIL and OPLS2009_0.8 force fields provide a better predictive capability in comparison to the other two force fields.

All the force fields indicate that the entropic driving force is either negligible or offers resistance to the dissolution of methane in the four ionic liquids. Among the force fields, a trend identical to that observed for the enthalpies of absorption can be noted for the entropy of absorption. For example, the application of the VSIL and OPLS2009_0.8 force field leads to values that are more aligned with the experimental data across the four ionic liquids, while CL&P and OPLS2009 force fields demonstrate a varying degree of agreement with the experimental observations. When a comparison is made with other gases in Table 2, it is can be seen that methane dissolution is least affected by entropic contributions.

Table 1: Comparison of Enthalpies of Absorption for Various Gases in Different Ionic liquids Obtained Using Different Force Field Models

	[C$_4$mim]Cl	[C$_4$mim][MeSO$_4$]	[C$_4$mim][NTf$_2$]	[C$_4$mim][DCA]
			Δh (kJ/mol)	
			CH_4	
CL&P*	−37.1 ± 5.4	−32.6 ± 9.8	−3.1 ± 2.1	5.8 ± 5.8
VSIL*	−2.8 ± 0.9	−4.1 ± 1.8	−2.7 ± 1.2	−2.8 ± 0.9
OPLS2009*	−30.9 ± 9.9	−59.6 ± 5.3	−11.2 ± 4.8	−0.3 ± 0.9
OPLS2009_0.8*	−5.3 ± 4.4	−0.1 ± 1.8	−2.5 ± 1.1	−0.5 ± 0.5
Kumelan et al. [92]†		−2.5 ± 0.0		
Pereira et al. [71]†				−1.7
Yu et al. [72]†			−1.7	
Yu et al. [73]†			−4.3	
			CO_2	
CL&P*	−35.1 ± 3.3	−16.1 ± 0.2	−15.0 ± 0.3	−15.5 ± 0.4
VSIL*	−13.0 ± 0.3	−14.4 ± 0.4	−12.9 ± 0.2	−14.0 ± 0.3
OPLS2009*	−41.4 ± 1.0	−22.6 ± 2.9	−10.6 ± 0.6	−12.8 ± 0.1
OPLS2009_0.8*	−13.8 ± 0.2	−13.3 ± 0.1	−12.8 ± 0.2	−14.5 ± 0.3
Jang et al. [75]†	−13.4 ± 0.1			
Kumelan et al. [77]†		−13.3		
Bahadur et al. [78]		−18.2 ± 4.5	−13.5 ± 1.8	
Anthony et al. [45]†			−12.5 ± 0.4	
Lee et al. [81]†			−13.0 ± 0.1	
Jacquemin et al. [39]†			−11.5 ± 0.6	
Hiraga et al. [82]†			−13.9	
Raeissi et al. [83]†			−13.1 ± 0.1	
Carvalho et al. [80]†			−15.9	−14.5
Singh et al. [52]			−13.0 ± 0.2	
			NH_3	
CL&P*	−47.6 ± 1.4	−21.6 ± 0.3	−16.5 ± 0.6	−25.6 ± 0.4
VSIL*	−25.3 ± 0.4	−17.6 ± 0.6	−14.3 ± 0.1	−18.5 ± 0.4
OPLS2009*	−47.6 ± 0.5	−4.3	−14.5 ± 0.5	−26.7 ± 0.6
OPLS2009_0.8*	−24.4 ± 0.3	−17.7 ± 0.4	−14.2 ± 0.2	−18.9 ± 0.1
			SO_2	
CL&P*	−63.4 ± 0.3	−41.5 ± 2.2	−26.0 ± 0.1	−24.8 ± 0.2
VSIL*	−23.1 ± 0.2	−24.5 ± 0.1	−23.2 ± 0.1	−23.1 ± 0.4
OPLS2009*	−71.2 ± 3.1	−43.0 ± 5.0	−18.1 ± 0.5	−25.9 ± 0.2
OPLS2009_0.8*	−20.3 ± 0.3	−24.5 ± 0.1	−24.4 ± 0.1	−23.7 ± 0.0
Huang et al. [43]			−21 ± 1	

* this work

† values extrapolated from the reported data

Table 2: Comparison of Entropies of Absorption for Various Gases in Different Ionic liquids Obtained Using Different Force Field Models

	[C_4mim]Cl	[C_4mim][$MeSO_4$]	[C_4mim][NTf_2]	[C_4mim][DCA]
			Δs (J/mol K)	
			CH_4	
CL&P*	−106.0 ± 15.2	−91.8 ± 27.3	−8.7 ± 6.0	16.2 ± 16.2
VSIL*	−7.9 ± 2.6	−11.6 ± 5.1	−7.7 ± 3.6	2.4 ± 2.6
OPLS2009*	−87.6 ± 28.6	−169.0 ± 14.4	−31.6 ± 13.6	−0.8 ± 2.7
OPLS2009_0.8*	−14.5 ± 12.5	−0.3 ± 4.9	−7.1 ± 3.1	−1.5 ± 1.4
Kumelan et al. [92]†		−7.0 ± 0.1		
Pereira et al. [71]†				−4.8
Yu et al. [72]†			−4.9	
Yu et al. [73]†			−12.5	
			CO_2	
CL&P*	−99.2 ± 9.9	−45.7 ± 0.2	−42.6 ± 1.2	−43.8 ± 1.3
VSIL*	−36.8 ± 0.6	−41.0 ± 1.2	−36.5 ± 0.3	−39.7 ± 1.1
OPLS2009*	−117.4 ± 3.6	−63.7 ± 8.5	−30.1 ± 1.3	−36.4 ± 0.1
OPLS2009_0.8*	−39.3 ± 0.3	−37.6 ± 0.6	−36.5 ± 0.4	−41.2 ± 1.1
Jang et al. [75]†	−37 ± 0.2			
Kumelan et al. [77]†		−37.7 ± 0.2		
Bahadur et al. [78]		−47.5 ± 5.5	−45.3 ± 5.7	
Anthony et al. [45]†			−41.3 ± 1.4	
Lee et al. [81]†			−42.2 ± 0.2	
Jacquemin et al. [39]†			−35.6 ± 2.0	
Hiraga et al. [82]†			−39.4 ± 0.3	
Raeissi et al. [83]†			−37.1 ± 0.4	
Carvalho et al. [80]†			−45.7 ± 0.2	−44.4 ± 0.2
Singh et al. [52]			−29.3 ± 3	
			NH_3	
CL&P*	−135.1 ± 4.7	−61.2 ± 1.1	−46.8 ± 1.8	−72.7 ± 1.4
VSIL*	−71.8 ± 1.4	−49.8 ± 1.8	−40.6 ± 0.1	−52.5 ± 0.8
OPLS2009*	−135.2 ± 2.1	−12.6 ± 6.8	−41.1 ± 1.7	−75.6 ± 2.1
OPLS2009_0.8*	−69.2 ± 0.4	−50.2 ± 1.5	−40.4 ± 0.3	−53.5 ± 0.1
			SO_2	
CL&P*	−179.9 ± 1.7	−117.5 ± 6.9	−74.0 ± 0.0	−70.4 ± 0.1
VSIL*	−65.5 ± 0.1	−69.7 ± 0.2	−65.8 ± 0.0	−65.6 ± 1.4
OPLS2009*	−202.6 ± 7.8	−121.3 ± 15.0	−51.2 ± 1.6	−73.6 ± 0.2
OPLS2009_0.8*	−57.7 ± 0.5	−69.6 ± 0.7	−69.2 ± 0.2	−67.2 ± 0.4
Huang et al. [43]			−61 ± 2	

* this work

† values extrapolated from the reported data

Table 3: Polarizabilities (α), Dipole Moments (μ) and Quadrupole Moments (Q) of the Gas Solutes

	$\alpha \times 10^{24}$ (cm^3) [93]	$\mu \times 10^{18}$ (esu * cm) [94]	$Q \times 10^{26}$ (esu * cm^2) [94]
CH_4	2.60	0.00	0.00
CO_2	2.64	0.00	−4.30
NH_3	2.22	+1.47	−1.00
SO_2	3.89	+1.61	+4.40

Taken together, we recommend the use of OPLS2009_0.8 and VSIL force fields for estimating the Henry's constants of CH_4 in the investigated ionic liquids. The temperature dependence of the Henry's constants, in the form of enthalpy and entropy of absorption, is correctly reproduced when comparison is carried out with the available experimental data. Although numerical values for the Henry's constants computed with the OPLS2009 and CL&P force field show varying degrees of agreement with the experimental data, the predictions of the enthalpy and entropy of absorption for [C_4mim][NTf_2] and [C_4mim][DCA] are found to be generally reliable.

4.2.2. CO_2

In comparison to the experimental value, the enthalpy of absorption for CO_2 in the ionic liquid [C_4mim]Cl is overpredicted by a factor of 2-3 when using the CL&P and OPLS2009 force fields, suggesting that the interaction between CO_2 and the ionic liquids modeled in these force fields is too strong. Based on the entropy of absorption, a much higher ordering in the ionic liquid is projected to occur by these force fields. The scaling of ionic charges by 0.8 (OPLS2009_0.8) results in the values of Δh and Δs closely matching the experimental measurements. The placement of an additional virtual site results into values that are indistinguishable from those obtained by simply scaling the charges. Thus, for [C_4mim]Cl, a correct temperature dependence can be expected when either the OPLS2009_0.8 or VSIL force field is applied. Given the spread in the experimental values for Δh and Δs, it is difficult to assess the accuracy of the simulation predictions for the ionic liquid [C_4mim][$MeSO_4$]. Nonetheless, it can be seen that the Δh and Δs predictions employing the force fields CL&P, OPLS2009_0.8, and VSIL are in very good agreement with experimental data. On the other hand, the CO_2-ionic liquid interactions are indicated to be slightly stronger than with the OPLS2009 force field. In the case of CO_2 in the ionic liquid [C_4mim][NTf_2], both Δh and Δs values are comparable across all the force fields and with experimental values. However, subtle differences do exist. For example, the CO_2-ionic liquid interactions are a little stronger in the CL&P force fields, while the interactions are marginally weaker in the OPLS2009 force field as suggested by Δh values. As a consequence of this behavior, the entropy of absorption is the most negative for the CL&P force field and the least for the OPLS2009 force field. Considering the dissolution of CO_2 in [C_4mim][DCA], the simulation results are in quantitative agreement with the experimental value for the enthalpy and entropy of absorption of CO_2 in the ionic liquid.

Overall, our analysis indicates that the OPLS2009_0.8 and VSIL force fields are to be preferred for estimating the temperature dependence of the Henry's constant of CO_2 in the four ionic liquids. We also conclude that, for CO_2, the effect of the additional virtual site in the VSIL force field is only secondary. The reduction of the CO_2-ionic liquid interaction by lowering the cation and anion charge to ± 0.8 is sufficient for predicting the behavior of the Henry's constant for CO_2 in these ionic liquids as a function of temperature. Another notable feature of these calculations is that the enthalpy and entropy of absorption calculated with the two force fields exhibit weak dependence on the type of ionic liquid, suggesting that the infinite dilution thermodynamics of CO_2 dissolution is similar in the four ionic liquids.

4.2.3. NH_3

The solubility mechanism of NH_3 in ionic liquids depends on the interaction of NH_3 with cation, which we believe has a non-negligible dependence on the interaction of cation with anions. As mentioned above, solubility of NH_3 in ionic liquids studied in this work follows the order Cl^- > [DCA]$^-$ > [$MeSO_4$]$^-$ > [NTf_2]$^-$, at a given temperature. The enthalpy and entropy of absorption for NH_3 determined with a given force field follows the identical order, implying that the physical mechanism underlying NH_3 solubility is captured by all the force fields. This observation is in contrast to that for CO_2 where Δh and Δs values are similar regardless of the ionic liquid being studied. It is interesting to note that the calculated enthalpy and entropy of absorption for $[C_4mim]Cl$ and $[C_4mim][DCA]$ with CL&P and OPLS2009 force fields are nearly identical, and consistently higher in magnitude when compared to the predictions from the OPLS2009_0.8 and VSIL force fields. For $[C_4mim][MeSO_4]$, almost no temperature dependence of the Henry's constant for NH_3 is indicated by very low enthalpy of absorption with OPLS2009 force field. As with CO_2, the enthalpy and entropy of absorption for each of the ionic liquids are within statistical uncertainties when predictions with OPLS2009_0.8 and VSIL are considered.

As no data for Δh and Δs are available for NH_3 for the four ionic liquids in the literature, comparison is carried out with other ionic liquids. For example, the calculated value of Δh from the works of Li et al. [50] for $[C_4mim][BF_4]$ is -18.6 ± 0.7 kJ/mol and those from the works of Yokozeki and Shiflett [49] for $[C_4mim][BF_4]$ and $[C_4mim][PF_6]$ are -24.6 ± 0.3 kJ/mol and -16.5 ± 0.2 kJ/mol, respectively. These values are comparable to those reported here for $[C_4mim][NTf_2]$. Further, the enthalpy of absorption based on the interaction energy of NH_3 with the cation and anion in $[C_2mim][NTf_2]$ computed by Shi and Maginn [59] is approximately -10 kJ/mol at 322 K. The enthalpies obtained in this work are higher possibly due to the additional van der Waals interactions contributed by the longer alkyl chain in $[C_4mim]^+$.

4.2.4. SO_2

An examination of the enthalpy of absorption data (Table 1) for SO_2 in various ionic liquids reveals that, as for CO_2, all the force fields predict similar values for the $[C_4mim][NTf_2]$ and $[C_4mim][DCA]$ while considerable differences exist for the other two ionic liquids. Furthermore, the OPLS2009_0.8 and VSIL force fields are in agreement with each other with the enthalpy of absorption between -20 kJ/mol to -24 kJ/mol for all the ionic liquids. The CL&P and OPLS2009 force fields predict strong temperature dependence of the Henry's constants with values approaching -60 to -70 kJ/mol for the $[C_4mim]Cl$ and -40 kJ/mol for the $[C_4mim][MeSO_4]$ ionic liquids. In comparison to the other gases, the interactions between SO_2 and the ionic liquids are found to be the strongest consistent with the very low values for the Henry's constants.

The entropy of absorption for SO_2 in all the ionic liquids are negative, indicating that entropic contributions disfavor the absorption of SO_2. As remarked for the enthalpy of absorption, the OPLS2009_0.8 and VSIL force fields lead to similar entropy of absorption (-60 to -70 J/mol K). All the force fields are in agreement with one another for $[C_4mim][DCA]$ and to some extent for $[C_4mim][NTf_2]$. The entropies of absorption calculated with CL&P and OPLS2009 force fields for $[C_4mim]Cl$ and $[C_4mim][MeSO_4]$ are lower (more negative) by a factor of 2-3 than the corresponding values determined for the OPLS2009_0.8 and VSIL force fields. The data for the Henry's constant for SO_2 along with the enthalpic and entropic contributions obtained with the four force fields suggest that the application of scaled charge models leads to better predictions.

5. Summary and Conclusion

We considered four all-atom ionic liquid force fields (two with integer charges and two with scaled charges of ± 0.8) to test their accuracy in predicting the Henry's constants of solutes of varying polarity in four ionic liquids: [C_4mim]Cl, [C_4mim][$MeSO_4$], [C_4mim][DCA] and [C_4mim][NTf_2]. The solutes of interest consisted of nonpolar CH_4, quadrupolar and acidic CO_2, and polar and basic NH_3 and polar and acidic SO_2. Henry's constants were determined by evaluating excess chemical potentials using BAR approach at temperatures of 333, 353, and 373 K. Partial molar enthalpies and entropies of absorption were derived from the temperature dependent Henry's constant using the van't Hoff equation.

Our calculations indicate that all the force fields are capable of reproducing the experimentally observed gas solubility trend ($SO_2 > NH_3 > CO_2 > CH_4$) in a given ionic liquid. This is remarkable considering that the Henry's constants span over three orders of magnitude. Similarly, the force fields can be employed to correctly identify ionic liquids with high gas solubility. For example, NH_3 solubility is ranked in the order of $Cl^- > [DCA]^- > [MeSO_4]^- > [NTf_2]^-$ which is the opposite to that found for CO_2 ($[NTf_2]^- > [DCA]^- > [MeSO_4]^- > Cl^-$). In addition, with a few exceptions, all the force fields show that the gas solubility decreases when the temperature is raised. As a consequence of which, we find that the entropies of absorption are negative for all the ionic liquids. Consistent with the solubility trends, the partial molar enthalpy of absorption are ordered (from least negative to the most) as $CH_4 < CO_2 < NH_3 < SO_2$. The partial molar entropies are also negative indicating enhanced ordering in the ionic liquids when these gases dissolve in the chosen ionic liquids.

In general, we find that the force fields with scaled charges (termed as VSIL and OPLS2009_0.8) tend to align better with experimental results in comparison to the integer charge models (OPLS2009 and CL&P). The reduction in the overall charge on the cation and anion also brings the enthalpies and entropies of absorption closer to the available literature data. As an aside, we note that the experimental data for NH_3 and SO_2 in ionic liquids are scarce when compared to those for CH_4 and CO_2. Such measurements will assist in expanding the present study to include more ionic liquids.

Acknowledgements

This material is based upon work supported by the National Science Foundation (NSF) Award Number CBET-1706978. The authors gratefully acknowledge partial funding from the Oklahoma State University. The computing for this project was performed at the OSU High Performance Computing Center at Oklahoma State University supported in part through the National Science Foundation grant OCI-1126330.

Supporting Information

Supporting information includes raw data of Henry's Law constants for CH_4, CO_2, NH_3 and SO_2 gases in [C_4mim]Cl, [C_4mim][$MeSO_4$], [C_4mim][DCA] and [C_4mim][NTf_2] ionic liquids at 333 K, 353 K and 373 K predicted using four different classical force fields.

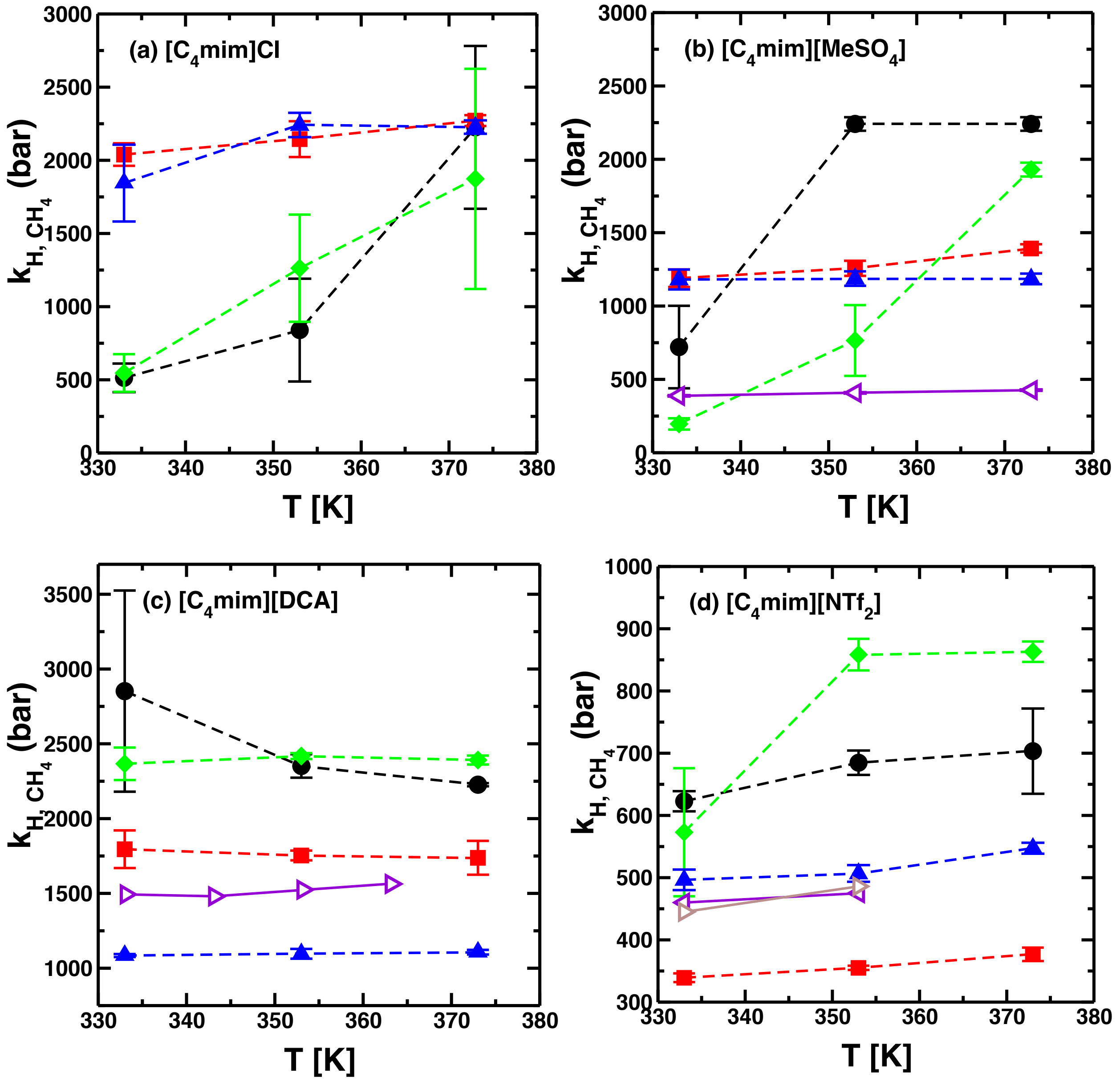

Figure 1: Comparison of Henry's constants predicted in this work using four different classical force fields - CL&P, VSIL, OPLS2009 and OPLS2009_0.8 - and available literature data for CH_4 in (a) [C_4mim]Cl (Legends: CL&P●, VSIL■, OPLS2009♦, OPLS2009_0.8 ▲); (b) [C_4mim][$MeSO_4$] (Legends: CL&P●, VSIL■, OPLS2009♦, OPLS2009_0.8 ▲, Kumelan et al. [92] (exp) ◁); (c) [C_4mim][DCA] (Legends: CL&P●, VSIL■, OPLS2009♦, OPLS2009_0.8 ▲, Pereira et al. [71] (exp) ▷); and (d) [C_4mim][NTf_2] (Legends: CL&P●, VSIL■, OPLS2009♦, OPLS2009_0.8 ▲, Yu et al. [72] (exp) ◁,Yu et al. [73] (sim) ▷) ionic liquids. Statistical uncertainties were calculated from three independent trials. Note that the lines joining data points are only guide to the eye.

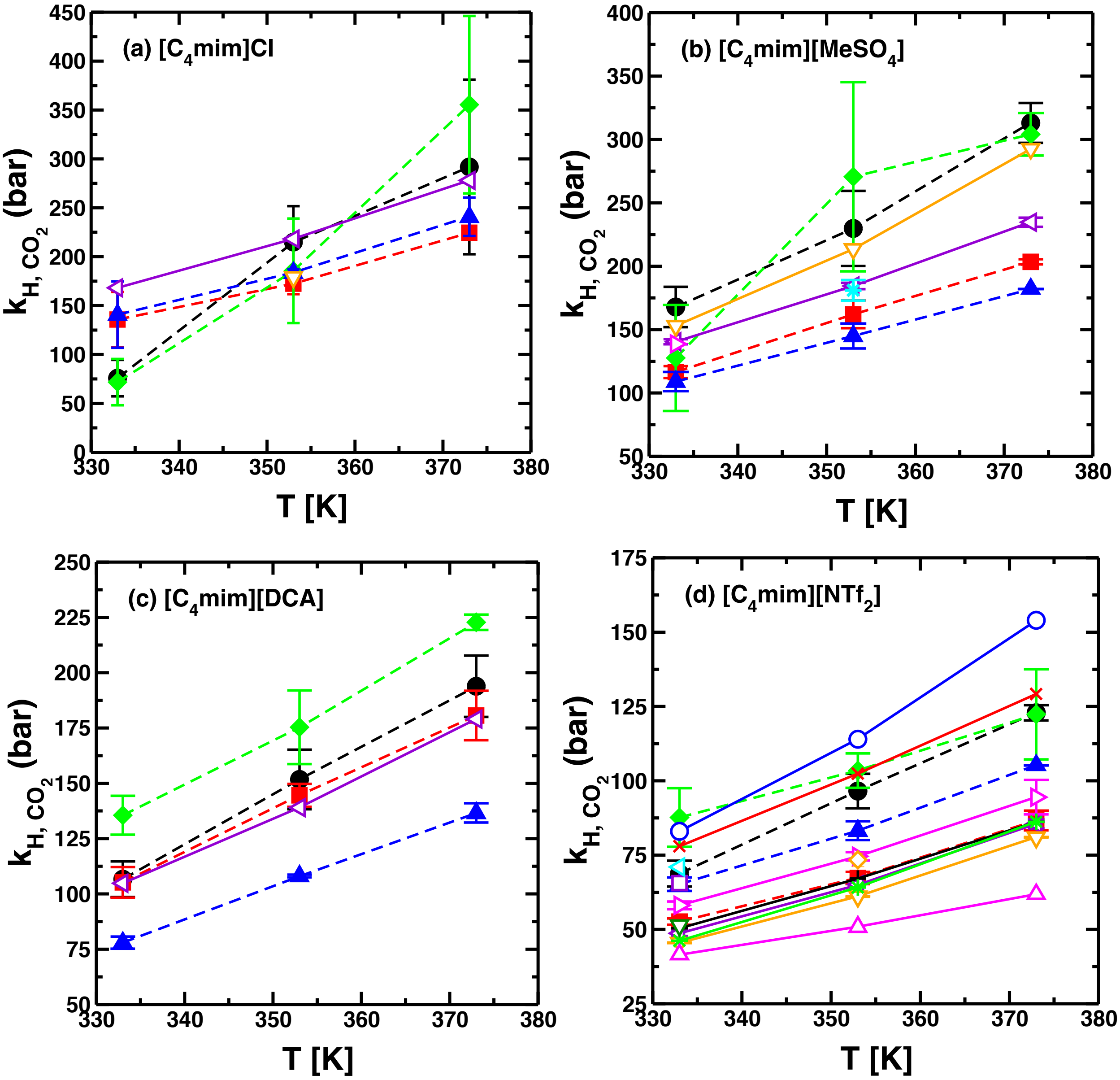

Figure 2: Comparison of Henry's constants predicted in this work using four different classical force fields - CL&P, VSIL, OPLS2009 and OPLS2009_0.8 - and available literature data for CO_2 in (a) [C$_4$mim]Cl (Legends: CL&P●, VSIL■, OPLS2009♦, OPLS2009_0.8 ▲, Jang et al. [75] (exp) ◁, Kapoor and Shah [76] (sim) ▽); (b) [C$_4$mim][MeSO$_4$] (Legends: CL&P●, VSIL■, OPLS2009♦, OPLS2009_0.8 ▲, Kumelan et al. [77] (exp) ◁, Bahadur et al. [78] (exp) ▽, Llovell et al. [79] (exp) ▷, Kapoor and Shah [76] (sim) ∗) ; (c) [C$_4$mim][DCA] (Legends: CL&P●, VSIL■, OPLS2009♦, OPLS2009_0.8 ▲, Carvalho et al. [80] (exp) ◁); and (d) [C$_4$mim][NTf$_2$] (Legends: CL&P●, VSIL■, OPLS2009♦, OPLS2009_0.8 ▲, Anthony et al. [45] (exp) ◁, Lee et al. [81] (exp) ▽, Jacquemin et al. [39] (exp) ▷, Hiraga et al. [82] (exp) +, Raeissi et al. [83] (exp) ×, Carvalho et al. [80] (exp) ∗, Bahadur et al. [78] (exp) ○, Ramdin et al. [57] (exp) □, Kapoor and Shah [76] (sim) ◇, Singh et al. [52] (sim) △, Ramdin et al. [57] (sim) ◁, Budhathoki et al. [51] (sim) ▽) ionic liquids. Statistical uncertainties were calculated from three independent trials. Note that the lines joining data points are only guide to the eye.

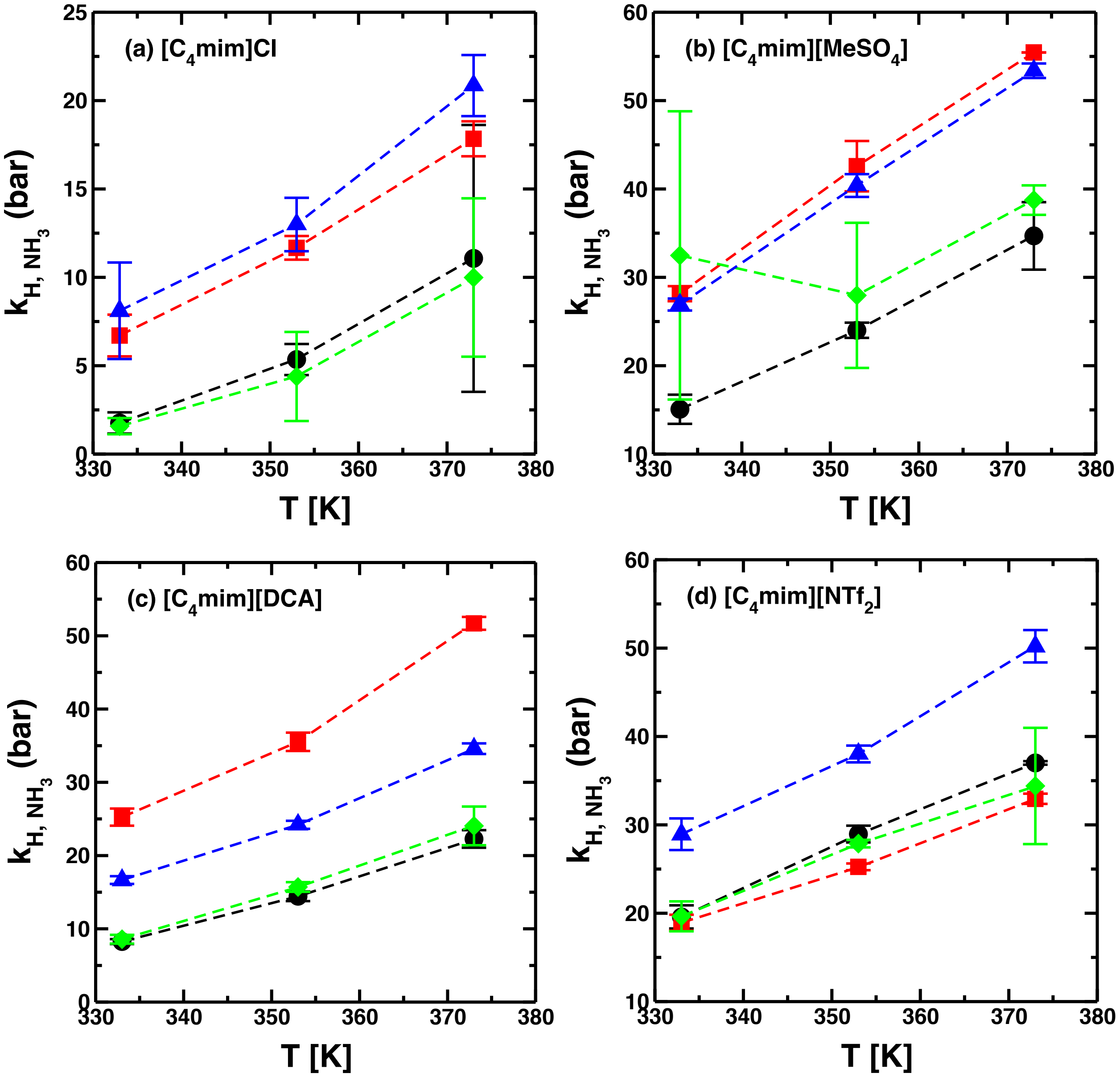

Figure 3: Comparison of Henry's constants predicted in this work using four different classical force fields - CL&P, VSIL, OPLS2009 and OPLS2009_0.8 - and available literature data for NH$_3$ in (a) [C$_4$mim]Cl (Legends: CL&P●, VSIL■, OPLS2009♦, OPLS2009_0.8 ▲); (b) [C$_4$mim][MeSO$_4$] (Legends: CL&P●, VSIL■, OPLS2009♦, OPLS2009_0.8 ▲); (c) [C$_4$mim][DCA] (Legends: CL&P●, VSIL■, OPLS2009♦, OPLS2009_0.8 ▲); and (d) [C$_4$mim][NTf$_2$] (Legends: CL&P●, VSIL■, OPLS2009♦, OPLS2009_0.8 ▲) ionic liquids. Statistical uncertainties were calculated from three independent trials. Note that the lines joining data points are only guide to the eye.

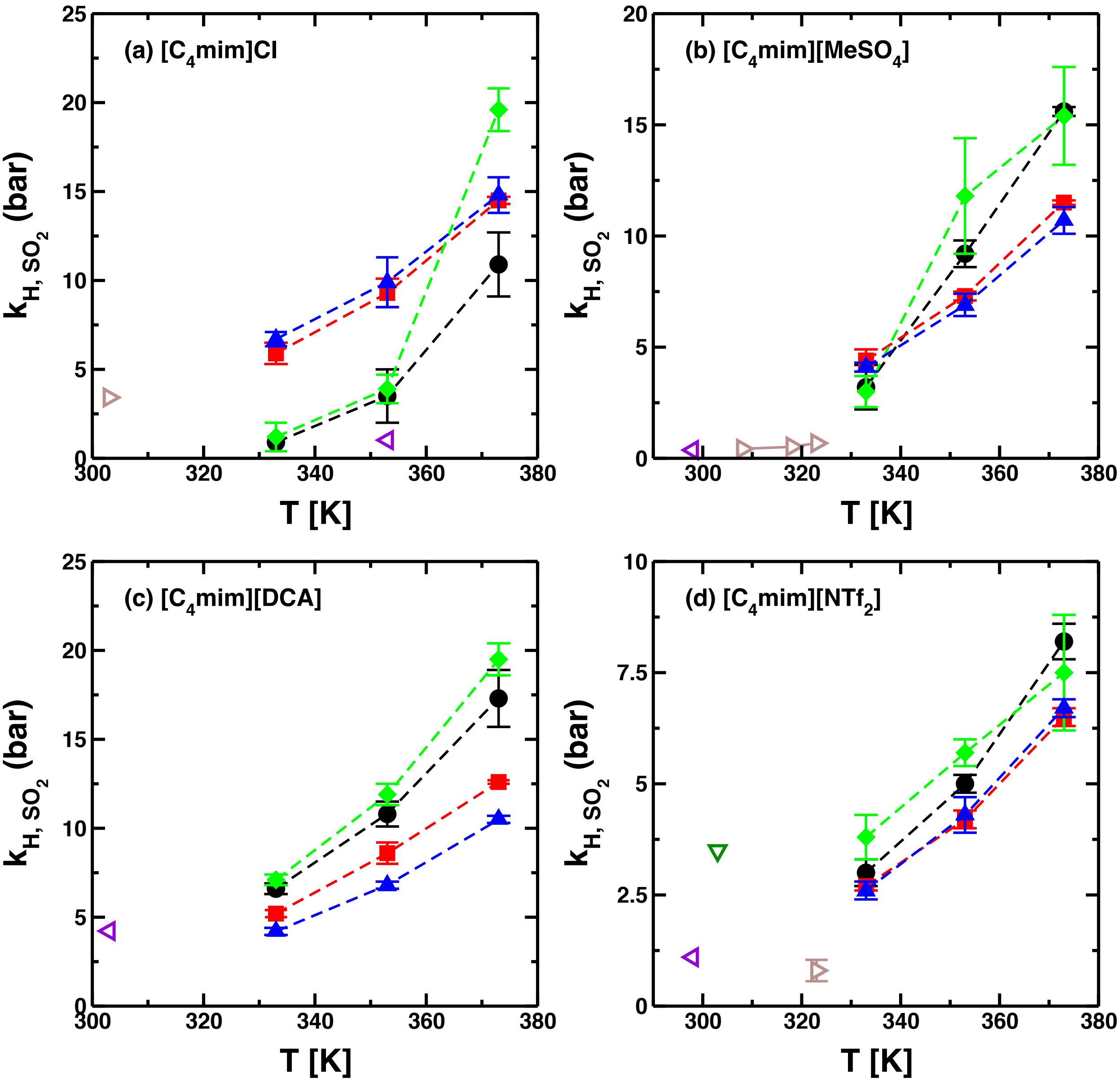

Figure 4: Comparison of Henry's Law constants predicted in this work using four different classical force fields - CL&P, VSIL, OPLS2009 and OPLS2009_0.8 - and available literature data for SO_2 in (a) [C_4mim]Cl (Legends: CL&P●, VSIL■, OPLS2009♦, OPLS2009_0.8 ▲, Mondal et al. [87] (exp) ◁, Garcia et al. [88] (sim) ▷); (b) [C_4mim][$MeSO_4$] (Legends: CL&P●, VSIL■, OPLS2009♦, OPLS2009_0.8 ▲, Shiflett & Yokozeki [44] (exp) ◁,Lee et al. [86] (exp) ▷); (c) [C_4mim][DCA] (Legends: CL&P●, VSIL■, OPLS2009♦, OPLS2009_0.8 ▲, Garcia et al. [88] (sim) ◁); and (d) [C_4mim][NTf_2] (Legends: CL&P●, VSIL■, OPLS2009♦, OPLS2009_0.8 ▲, Dai et al. [91] (exp) ◁, Garcia et al. [88] (sim) ▷, Garcia et al. [88] (sim) ▽, Ghobadi et al. [95] (exp) ▷) ionic liquids. Statistical uncertainties were calculated from three independent trials. Note that the lines joining data points are only guide to the eye.

References

[1] F. Endres, S. Zein El Abedin, Air and Water Stable Ionic Liquids in Physical Chemistry, Phys. Chem. Chem. Phys. 8 (18) (2006) 2101–16.

[2] M. Galiński, A. Lewandowski, I. Stépniak, Ionic Liquids as Electrolytes, Electrochim. Acta 51 (26) (2006) 5567–5580.

[3] R. Lin, P.-L. Taberna, S. Fantini, V. Presser, C. R. Pérez, F. Malbosc, N. L. Rupesinghe, K. B. K. Teo, Y. Gogotsi, P. Simon, Capacitive Energy Storage from –50 to 100 ^{0}C Using an Ionic Liquid Electrolyte, J. Phys. Chem. Lett. 2 (19) (2011) 2396–2401.

[4] D. R. MacFarlane, N. Tachikawa, M. Forsyth, J. M. Pringle, P. C. Howlett, G. D. Elliott, J. H. Davis, M. Watanabe, P. Simon, C. A. Angell, Energy Applications of Ionic Liquids, Energy Environ. Sci. 7 (1) (2014) 232–250.

[5] P. Wasserscheid, W. Keim, Ionic Liquids - New “Solutions” for Transition Metal Catalysis, Angewandte Chemie International Edition 39 (2000) 3772–3789.

[6] A. Riisager, R. Fehrmann, M. Haumann, P. Wasserscheid, Supported Ionic Liquids: Versatile Reaction and Separation Media, Top Catal. 40 (1-4) (2006) 91–102.

[7] G. H. Lane, P. M. Bayley, B. R. Clare, A. S. Best, D. R. MacFarlane, M. Forsyth, A. F. Hollenkamp, Ionic Liquid Electrolyte for Lithium Metal Batteries: Physical, Electrochemical, and Interfacial Studies of N-Methyl- N-butylmorpholinium Bis(fluorosulfonyl)imide, J. Phys. Chem. C 114 (49) (2010) 21775–21785.

[8] L. T. Costa, B. Sun, F. Jeschull, D. Brandell, Polymer-Ionic Liquid Ternary Systems for Li-Battery Electrolytes: Molecular Dynamics Studies of LiTFSI in a Emim-TFSI and Peo Blend, J. Chem. Phys. 143 (2) (2015) 024904–10.

[9] A. Basile, H. Yoon, D. R. MacFarlane, M. Forsyth, P. C. Howlett, Investigating Non-Fluorinated Anions for Sodium Battery Electrolytes Based on Ionic Liquids, Electrochem. Commun. 71 (C) (2016) 48–51.

[10] J. Szymczak, S. Legeai, S. Michel, S. Diliberto, N. Stein, C. Boulanger, Electrodeposition of Stoichiometric Bismuth Telluride Bi_2Te_3 Using A Piperidinium Ionic Liquid Binary Mixture, Electrochim. Acta 137 (2014) 586–594.

[11] Z. Liu, T. Cui, T. Lu, M. Shapouri Ghazvini, F. Endres, Anion Effects on the Solid/Ionic Liquid Interface and the Electrodeposition of Zinc, J. Phys. Chem. C 120 (36) (2016) 20224–20231.

[12] P. Wang, S. M. Zakeeruddin, J.-E. Moser, M. Grätzel, A New Ionic Liquid Electrolyte Enhances the Conversion Efficiency of Dye-Sensitized Solar Cells, J. Phys. Chem. B 107 (48) (2003) 13280–13285.

[13] C. Pinilla, M. G. Del Pópolo, R. M. Lynden-Bell, J. Kohanoff, Structure and Dynamics of a Confined Ionic Liquid. Topics of Relevance to Dye-Sensitized Solar Cells, J. Phys. Chem. B 109 (38) (2005) 17922–17927.

[14] M. Bidikoudi, T. Stergiopoulos, V. Likodimos, G. E. Romanos, M. Francisco, B. Iliev, G. Adamová, T. J. S. Schubert, P. Falaras, Ionic Liquid Redox Electrolytes Based on Binary Mixtures of 1-Alkyl-Methylimidazolium Tricyanomethanide With 1-Methyl-3-Propylimidazolium Iodide and Implication In Dye-Sensitized Solar Cells, J. Mater. Chem. A 1 (35) (2013) 10474–13.

[15] J. L. Anthony, E. J. Maginn, J. F. Brennecke, Solubilities and Thermodynamic Properties of Gases in the Ionic Liquid 1-n-Butyl-3-methylimidazolium Hexafluorophosphate, J. Phys. Chem. B 106 (29) (2002) 7315–7320.

[16] J. E. Bara, T. K. Carlisle, C. J. Gabriel, D. Camper, A. Finotello, D. L. Gin, R. D. Noble, Guide to CO_2 Separations in Imidazolium-Based Room-Temperature Ionic Liquids, Ind. Eng. Chem. Res. 48 (6) (2009) 2739–2751.

[17] D. Almantariotis, S. Stevanovic, O. Fandiño, A. S. Pensado, A. A. H. Pádua, J. Y. Coxam, M. F. Costa Gomes, Absorption of Carbon Dioxide, Nitrous Oxide, Ethane and Nitrogen by 1-Alkyl-3-methylimidazolium (C nmim, n= 2,4,6) Tris(pentafluoroethyl)trifluorophosphate Ionic Liquids (eFAP), J. Phys. Chem. B 116 (26) (2012) 7728–7738.

[18] Z. Lei, C. Dai, B. Chen, Gas Solubility in Ionic Liquids, Chem. Rev. 114 (2) (2014) 1289–1326.

[19] N. V. Plechkova, K. R. Seddon, Applications of Ionic Liquids in the Chemical Industry, Chem. Soc. Rev. 37 (2008) 123–150.

[20] U. Kapoor, J. K. Shah, Preferential Ionic Interactions and Microscopic Structural Changes Drive Nonideality in Binary Ionic Liquid Mixtures as Revealed from Molecular Simulations, Ind. Eng. Chem. Res. 55 (51) (2016) 13132–13146.

[21] U. Kapoor, J. K. Shah, Thermophysical Properties of Imidazolium-Based Binary Ionic Liquid Mixtures Using Molecular Dynamics Simulations, J. Chem. Eng. Data 63 (7) (2018) 2512–2521.

[22] G. Chatel, J. Pereira, V. Debbeti, R. D. Wang, H.and Rogers, Mixing ionic liquids – “simple mixtures” or “double salts”?, Green Chem. 16 (4) (2014) 2051–33.

[23] R. P. Matthews, I. Villar-Garcia, C. C. Weber, J. Griffith, F. Cameron, J. P. Hallett, P. A. Hunt, T. Welton, A Structural Investigation of Ionic Liquid Mixtures, Phys. Chem. Chem. Phys. 18 (12) (2016) 8608–8624.

[24] J. N. Canongia Lopes, J. Deschamps, A. A. H. Pádua, Modeling Ionic Liquids Using a Systematic All-Atom Force Field, J. Phys. Chem. B 108 (30) (2004) 11250–11250.

[25] J. N. Canongia Lopes, A. A. H. Pádua, Molecular Force Field for Ionic Liquids Composed of Triflate or Bistriflylimide Anions, J. Phys. Chem. B 108 (43) (2004) 16893–16898.

[26] J. N. Canongia Lopes, A. A. H. Pádua, Molecular Force Field for Ionic Liquids III: Imidazolium, Pyridinium, and Phosphonium Cations; Chloride, Bromide, and Dicyanamide Anions, J. Phys. Chem. B 110 (39) (2006) 19586–19592.

[27] J. N. Canongia Lopes, A. A. H. Pádua, K. Shimizu, Molecular Force Field for Ionic Liquids IV: Trialkylimidazolium and Alkoxycarbonyl-Imidazolium Cations; Alkylsulfonate and Alkylsulfate Anions, J. Phys. Chem. B 112 (16) (2008) 5039–5046.

[28] S. V. Sambasivarao, O. Acevedo, Development of OPLS-AA Force Field Parameters for 68 Unique Ionic Liquids, J. Chem. Theory Comput. 5 (4) (2009) 1038–1050.

[29] B. Doherty, X. Zhong, S. Gathiaka, B. Li, O. Acevedo, Revisiting OPLS Force Field Parameters for Ionic Liquid Simulations, J. Chem. Theory Comput. 13 (12) (2017) 6131–6145.

[30] B. Doherty, X. Zhong, O. Acevedo, Virtual Site OPLS Force Field for Imidazolium-Based Ionic Liquids, J. Phys. Chem. B 122 (11) (2018) 2962–2974.

[31] T. Köddermann, D. Paschek, R. Ludwig, Molecular Dynamic Simulations of Ionic Liquids: A Reliable Description of Structure, Thermodynamics and Dynamics, Chem. Phys. Chem. 8 (17) (2007) 2464–2470.

[32] J. Neumann, B. Golub, L.-M. Odebrecht, R. Ludwig, D. Paschek, Revisiting Imidazolium Based Ionic Liquids: Effect of The Conformation Bias of The [NTf_2] Anion Studied By Molecular Dynamics Simulations, J. Chem. Phys. 148 (19) (2018) 193828–10.

[33] C. Cadena, E. Maginn, Molecular Simulation Study of Some Thermophysical and Transport Properties of Triazolium-Based Ionic Liquids, J. Phys. Chem. B 110 (36) (2006) 18026–18039.

[34] K. E. Gutowski, B. Gurkan, E. J. Maginn, Force Field for the Atomistic Simulation of the Properties of Hydrazine, Organic Hydrazine Derivatives, and Energetic Hydrazinium Ionic Liquids, Pure Appl. Chem. 81 (10) (2009) 1799–1828.

[35] H. Liu, E. Maginn, A Molecular Dynamics Investigation of the Structural and Dynamic Properties of the Ionic Liquid 1-n-butyl-3-methylimidazolium bis(trifluoromethanesulfonyl)imide, J. Chem. Phys. 135 (12) (2011) 124507.

[36] Y. Zhang, E. J. Maginn, A Simple AIMD Approach to Derive Atomic Charges for Condensed Phase Simulation of Ionic Liquids, J. Phys. Chem. B 116 (33) (2012) 10036–10048.

[37] Y. Zhang, E. J. Maginn, Direct Correlation between Ionic Liquid Transport Properties and Ion Pair Lifetimes: A Molecular Dynamics Study, J. of Phys. Chem. Lett. 6 (4) (2015) 700–705.

[38] L. A. Blanchard, D. Hancu, E. J. Beckman, J. F. Brennecke, Green Processing Using Ionic Liquids and CO_2, Nature 399 (6731) (1999) 28–29.

[39] J. Jacquemin, P. Husson, V. Majer, M. F. Costa Gomes, Influence of the Cation on the Solubility of CO_2 and H_2 in Ionic Liquids Based on the Bis(trifluoromethylsulfonyl)imide Anion, J. Solution Chem. 36 (8) (2007) 967–979.

[40] J. L. Anderson, J. K. Dixon, J. F. Brennecke, Solubility of CO_2, CH_4, C_2H_6, C_2H_4, O_2, and N_2 in 1-Hexyl-3-methylpyridinium Bis(trifluoromethylsulfonyl)imide: Comparison to Other Ionic Liquids, Acc. Chem. Res. 40 (11) (2007) 1208–1216.

[41] M. a. D. Bermejo, T. M. Fieback, Á. Martín, Solubility of Gases In 1-Alkyl-3-Methylimidazolium Alkyl Sulfate Ionic Liquids: Experimental Determination and Modeling, J. Chem. Thermodyn. 58 (C) (2013) 237–244.

[42] Y.-Y. Jiang, Z. Zhou, Z. Jiao, L. Li, Y.-T. Wu, Z.-B. Zhang, SO_2 Gas Separation Using Supported Ionic Liquid Membranes, J. Phys. Chem. B 111 (19) (2007) 5058–5061.

[43] J. Huang, A. Riisager, R. W. Berg, R. Fehrmann, Tuning Ionic Liquids for High Gas Solubility and Reversible Gas Sorption, J. Mol. Catal. A: Chem. 279 (2) (2008) 170–176.

[44] M. B. Shiflett, A. Yokozeki, Chemical Absorption of Sulfur Dioxide in Room-Temperature Ionic Liquids, Ind. Eng. Chem. Res. 49 (3) (2010) 1370–1377.

[45] J. L. Anthony, J. L. Anderson, E. J. Maginn, J. F. Brennecke, Anion Effects on Gas Solubility in Ionic Liquids, J. Phys. Chem. B 109 (13) (2005) 6366–6374.

[46] A. H. Jalili, M. Rahmati-Rostami, C. Ghotbi, M. Hosseini-Jenab, A. N. Ahmadi, Solubility of H_2S in Ionic Liquids [bmim][PF_6], [bmim][BF_4], and [bmim][Tf_2N], J. Chem. Eng. Data 54 (6) (2009) 1844–1849.

[47] H. Sakhaeinia, V. Taghikhani, A. H. Jalili, A. Mehdizadeh, A. A. Safekordi, Solubility of H_2S in 1-(2-Hydroxyethyl)-3-Methylimidazolium Ionic Liquids With Different Anions, Fluid Phase Equilib. 298 (2) (2010) 303–309.

[48] A. Yokozeki, M. B. Shiflett, Vapor–Liquid Equilibria of Ammonia+Ionic Liquid Mixtures, Appl. Energy 84 (12) (2007) 1258–1273.

[49] A. Yokozeki, M. B. Shiflett, Ammonia Solubilities in Room-Temperature Ionic Liquids, Ind. Eng. Chem. Res. 46 (5) (2007) 1605–1610.

[50] G. Li, Q. Zhou, X. Zhang, LeiWang, S. Zhang, J. Li, Solubilities of Ammonia in Basic Imidazolium Ionic Liquids, Fluid Phase Equilib. 297 (1) (2010) 34–39.

[51] S. Budhathoki, J. K. Shah, E. J. Maginn, Molecular Simulation Study of the Solubility, Diffusivity and Permselectivity of Pure and Binary Mixtures of CO_2 and CH_4 in the Ionic Liquid 1-n-Butyl-3-methylimidazolium bis(trifluoromethylsulfonyl)imide, Ind. Eng. Chem. Res. 54 (35) (2015) 8821–8828.

[52] R. Singh, E. Marin-Rimoldi, E. J. Maginn, A Monte Carlo Simulation Study To Predict the Solubility of Carbon Dioxide, Hydrogen, and Their Mixture in the Ionic Liquids 1-Alkyl-3-methylimidazolium bis(trifluoromethanesulfonyl)amide ([$C_n$mim][Tf_2N], n= 4, 6), Ind. Eng. Chem. Res. 54 (16) (2015) 4385–4395.

[53] X. Zhang, F. Huo, Z. Liu, W. Wang, W. Shi, E. Maginn, Absorption of CO_2 in the Ionic Liquid 1-n-Hexyl-3-methylimidazolium Tris (pentafluoroethyl) trifluorophosphate ([hmim][FEP]): A Molecular View by Computer Simulations, J. Phys. Chem. B 113 (21) (2009) 7591–7598.

[54] W. Shi, E. Maginn, Molecular Simulation and Regular Solution Theory Modeling of Pure and Mixed Gas Absorption in the Ionic Liquid 1-n-Hexyl-3-methylimidazolium Bis (Trifluoromethylsulfonyl) amide ([hmim][Tf2N]), J. Phys. Chem. B 112 (2008) 16710–16720.

[55] W. Shi, E. J. Maginn, Atomistic Simulation of the Absorption of Carbon Dioxide and Water in the Ionic Liquid 1-n-hexyl-3-methylimidazolium bis(trifluoromethylsulfonyl)imide ([hmim][Tf2N], J. Phys. Chem. B 112 (7) (2008) 2045–2055.

[56] J. K. Shah, E. J. Maginn, Monte Carlo Simulations of Gas Solubility in the Ionic Liquid 1-n-butyl-3-methylimidazolium hexafluorophosphate., J. Phys. Chem. B 109 (20) (2005) 10395–10405.

[57] M. Ramdin, S. P. Balaji, J. M. Vicent-Luna, J. J. Gutiérrez-Sevillano, S. Calero, T. W. de Loos, T. J. H. Vlugt, Solubility of the Precombustion Gases CO_2, CH_4, CO, H_2, N_2, and H_2S in the Ionic Liquid [bmim][Tf_2N] from Monte Carlo Simulations, J. Phys. Chem. C 118 (41) (2014) 23599–23604.

[58] M. Ramdin, Q. Chen, S. P. Balaji, J. M. Vicent-Luna, A. Torres-Knoop, D. Dubbeldam, S. Calero, T. W. de Loos, T. J. H. Vlugt, Solubilities of CO_2, CH_4, C_2H_6, and SO_2 in ionic liquids and Selexol from Monte Carlo simulations, J. Comput. Phys. 15 (2016) 74–80.

[59] W. Shi, E. J. Maginn, Molecular Simulation of Ammonia Absorption in the Ionic Liquid 1-Ethyl-3-Methylimidazolium Bis(Trifluoromethylsulfonyl)Imide ([emim][Tf_2N]), AIChE J. 55 (9) (2009) 2414–2421.

[60] T. M. Becker, M. Wang, A. Kabra, S. H. Jamali, M. Ramdin, D. Dubbeldam, C. A. Infante Ferreira, T. J. H. Vlugt, Absorption Refrigeration Cycles with Ammonia–Ionic Liquid Working Pairs Studied by Molecular Simulation, Ind. Eng. Chem. Res. 57 (15) (2018) 5442–5452.

[61] E. Marin-Rimoldi, J. K. Shah, E. M. F. P. Equilibria, 2016, Monte Carlo Simulations of Water Solubility in Ionic Liquids: A Force Field Assessment, Fluid Phase Equilib. 407 (2016) 117–125.

[62] R. Lungwitz, S. Spange, A Hydrogen Bond Accepting (HBA) Scale For Anions, Including Room Temperature Ionic Liquids, New J. Chem. 32 (3) (2008) 392–3.

[63] R. Lungwitz, V. Strehmel, S. Spange, The Dipolarity/Polarisability of 1-Alkyl-3-Methylimidazolium Ionic Liquids as Function of Anion Structure and the Alkyl Chain Length, New J. Chem. 34 (6) (2010) 1135–6.

[64] W. Shi, E. J. Maginn, Atomistic Simulation of the Absorption of Carbon Dioxide and Water in the Ionic Liquid 1-n-Hexyl-3-methylimidazolium Bis(trifluoromethylsulfonyl)imide ([hmim][Tf_2N], J. Phys. Chem. B 112 (7) (2008) 2045–2055.

[65] W. Shi, E. J. Maginn, Improvement in Molecule Exchange Efficiency in Gibbs Ensemble Monte Carlo: Development and Implementation of the Continuous Fractional Component Move, J. Comput. Chem. 29 (15) (2008) 2520–2530.

[66] M. Martin, J. Siepmann, Transferable Potentials for Phase Equilibria. 1. United-Atom Description of n-Alkanes, J. Phys. Chem. B 102 (14) (1998) 2569–2577.

[67] E. Lindahl, B. Hess, D. van der Spoel, GROMACS 3.0: A Package for Molecular Simulation and Trajectory Analysis, Molec. Model. Ann. 7 (8) (2001) 306–317.

[68] M. J. Abraham, D. van der Spoel, E. Lindahl, B. Hess, t. G. d. team, GROMACS User Manual Version 5.0.4, www.gromacs.org, J. Mol. Model.

[69] C. H. Bennett, Efficient Estimation of Free Energy Differences from Monte Carlo Data, J. Comput. Phys. 22 (1976) 245–268.

[70] L. Martínez, R. Andrade, E. G. Birgin, J. M. Martínez, PACKMOL: A Package for Building Initial Configurations for Molecular Dynamics Simulations, J. Comput. Chem. 30 (13) (2009) 2157–2164.

[71] L. M. Pereira, V. Martins, K. A. Kurnia, M. B. Oliveira, A. M. Dias, F. Llovell, L. F. Vega, P. J. Carvalho, J. A. Coutinho, High pressure solubility of CH_4, N_2O and N_2 in 1-butyl-3-methylimidazolium dicyanamide: Solubilities, selectivities and soft-SAFT modeling, J. Supercrit. Fluids 110 (2016) 56–64.

[72] G. Yu, C. Dai, L. Wu, Z. Lei, Natural Gas Dehydration with Ionic Liquids, Energy Fuels 31 (2) (2017) 1429–1439.

[73] G. Yu, C. Dai, Z. Lei, Modified UNIFAC-Lei Model for Ionic Liquid-CH_4 Systems, Ind. Eng. Chem. Res. 57 (20) (2018) 7064–7076.

[74] S. Raeissi, C. J. Peters, High Pressure Phase Behaviour of Methane in 1-butyl-3-methylimidazolium bis(trifluoromethylsulfonyl)imide, Fluid Phase Equilib. 294 (1-2) (2010) 67–71.

[75] S. Jang, D.-W. Cho, T. Im, H. Kim, High-Pressure Phase Behavior of CO_2 + 1-Butyl-3-Methylimidazolium Chloride System, Fluid Phase Equilib. 299 (2) (2010) 216–221.

[76] U. Kapoor, J. K. Shah, Molecular Origins of the Apparent Ideal CO_2 Solubilities in Binary Ionic Liquid Mixtures, J. Phys. Chem. B 122 (42) (2018) 9763–9774.

[77] J. Kumełan, Á. Pérez-Salado Kamps, D. Tuma, G. Maurer, Solubility of CO_2 in the Ionic Liquids [bmim][CH_3SO_4] and [bmim][PF_6], J. Chem. Eng. Data 51 (5) (2006) 1802–1807.

[78] I. Bahadur, K. Osman, C. Coquelet, P. Naidoo, D. Ramjugernath, Solubilities of Carbon Dioxide and Oxygen in the Ionic Liquids Methyl Trioctyl Ammonium Bis(trifluoromethylsulfonyl)imide, 1-Butyl-3-Methyl Imidazolium Bis(trifluoromethylsulfonyl)imide, and 1-Butyl-3-Methyl Imidazolium Methyl Sulfate, J. Phys. Chem. B 119 (4) (2015) 1503–1514.

[79] F. Llovell, M. B. Oliveira, J. A. P. Coutinho, L. F. Vega, Solubility of Greenhouse and Acid Gases on the [C_4mim][$MeSO_4$] Ionic Liquid for Gas Separation and CO_2 Conversion, Catal. Today 255 (2015) 87–96.

[80] P. J. Carvalho, V. H. Álvarez, I. M. Marrucho, M. Aznar, J. A. P. Coutinho, High Pressure Phase Behavior of Carbon Dioxide in 1-Butyl-3-Methylimidazolium Bis(Trifluoromethylsulfonyl)Imide and 1-Butyl-3-Methylimidazolium Dicyanamide Ionic Liquids, J. Supercrit. Fluids 50 (2) (2009) 105–111.

[81] B.-C. Lee, S. L. Outcalt, Solubilities of Gases in the Ionic Liquid 1-n-Butyl-3-methylimidazolium Bis(trifluoromethylsulfonyl)imide, J. Chem. Eng. Data 51 (3) (2006) 892–897.

[82] Y. Hiraga, K. Koyama, Y. Sato, R. L. Smith Jr., Measurement and Modeling of CO_2 Solubility in [bmim]Cl – [bmim][Tf_2N] Mixed-Ionic Liquids For Design of Versatile Reaction Solvents, J. Supercrit. Fluids 132 (2018) 42–50.

[83] S. Raeissi, C. J. Peters, Carbon Dioxide Solubility in the Homologous 1-Alkyl-3-methylimidazolium Bis(trifluoromethylsulfonyl)imide Family , J. Chem. Eng. Data 54 (2) (2009) 382–386.

[84] P. Husson-Borg, V. Majer, M. F. Costa Gomes, Solubilities of Oxygen and Carbon Dioxide in Butyl Methyl Imidazolium Tetrafluoroborate as a Function of Temperature and at Pressures Close to Atmospheric Pressure , J. Chem. Eng. Data 48 (3) (2003) 480–485.

[85] Z. Liu, T. Chen, A. Bell, B. Smit, Improved United-Atom Force Field for 1-Alkyl-3-methylimidazolium Chloride, J. Phys. Chem. B 114 (13) (2010) 4572–4582.

[86] K. Lee, G. Gonga, H. Song, C. S. K. Honggon Kima, Kwang-Deog Junga, Use of Ionic Liquids as Absorbents To Separate SO_2 in SO_2/O_2 in Thermochemical Processes to Produce Hydrogen, Int. J. Hydrogen Energy 33 (21) (2008) 6031–6036.

[87] A. Mondal, S. Balasubramanian, Understanding SO_2 Capture by Ionic Liquids, J. Phys. Chem. B 120 (19) (2016) 4457–4466.

[88] G. García, M. Atilhan, S. Aparicio, A Density Functional Theory Insight Towards The Rational Design of Ionic Liquids For SO_2 Capture, Phys. Chem. Chem. Phys. 17 (20) (2015) 13559–13574.

[89] J. L. Anderson, J. K. Dixon, E. J. Maginn, J. F. Brennecke, Measurement of SO_2 Solubility in Ionic Liquids, J. Phys. Chem. B 110 (31) (2006) 15059–15062.

[90] W. Shi, E. J. Maginn, Molecular simulation and regular solution theory modeling of pure and mixed gas absorption in the ionic liquid 1-n-hexyl-3-methylimidazolium bis(trifluoromethylsulfonyl)amide ([hmim][tf_2n]), J. Phys. Chem. B. 112 (2008) 16710–16720.

[91] C. Dai, Z. Lei, B. Chen, Predictive Thermodynamic Models for Ionic Liquid-SO_2 Systems, Ind. Eng. Chem. Res. 54 (43) (2015) 10910–10917.

[92] J. Kumełan, Á. P. S. Kamps, D. Tuma, G. Maurer, Solubility of the Single Gases Methane and Xenon in the Ionic Liquid [bmim][CH_3SO_4], J. Chem. Eng. Data 52 (6) (2007) 2319–2324.

[93] J. M. Prausnitz, R. N. Lichtenthaler, E. G. de Azevedo, Molecular Thermodynamics of Fluid-Phase Equilibria, 3rd Edition, Prentice Hall, 1999.

[94] D. E. Stogryn, A. P. Stogryn, Molecular multipole moments, Mol. Phys. 11 (4) (1966) 371–393.

[95] A. F. Ghobadi, V. Taghikhani, J. R. Elliott, Investigation on the Solubility of SO_2 and CO_2 in Imidazolium-Based Ionic Liquids Using NPT Monte Carlo Simulation, J. Phys. Chem. B 115 (46) (2011) 13599–13607.